Full Paper

Journal of the Brazilian Chemical Society

https://dx.doi.org/10.21577/0103-5053.20250042

J. Braz. Chem. Soc. **2025**, *36*, 6, e-20250042, 1-9

New Colletotricandins and Thielavins Isolated from *Colletotrichum gloeosporioides*

Mustapha N. Abubakar, [a] ***Vitor S. Mazucato*** [a] ***and Paulo C. Vieira*** *,[a]

[a]*Departamento de Ciências BioMoleculares, Faculdade de Ciências Farmacêuticas de Ribeirão Preto, Universidade de São Paulo, 14040-903 Ribeirão Preto-SP, Brazil*

This study investigates the chemical diversity and compares the metabolites of *Colletotrichum gloeosporioides* extracted from potato dextrose broth (PDB) and rice media. *C. gloeosporioides* is a fungal pathogen known for compromising protease-rich edible fruits, such as papaya. Comparative analyses of the ethyl acetate extracts using ^{1}H nuclear magnetic resonance (NMR) spectroscopy and gas chromatography-mass spectrometry (CG-MS) reveal significant variations in chemical diversity and enhanced metabolite production in rice media compared to PDB. High-performance liquid chromatographic technique applied to the rice ethyl acetate extract led to the identification of two new derivatives of colletotricandin, designated C and D, as well as two additional derivatives of thielavin, named 3-demethylthielavin M and 3",3'-didemethyl-3-methylthielavin N. These newly identified compounds were thoroughly analyzed alongside previously known metabolites. The structure elucidation of the compounds was performed using NMR, high-resolution mass spectrometry (HR-MS), and GC-MS spectroscopy.

Keywords: *Colletotrichum gloeosporioides*, pathogens, colletotricandins, thielavins, metabolites

Introduction

Colletotrichum gloeosporioides is a well-known plant pathogen responsible for anthracnose, a prevalent disease affecting protease-rich edible fruits such as papaya, pineapple, and persimmon. This pathogen is characterized by dark, sunken lesions on various plant parts, including leaves, stems, and flowers.[1-4] Its pathogenicity effects lead to defoliation, premature fruit drop, and a general decline in plant health and productivity. Adaptable and widely transmitted through soil, wind, water, and human activities, *C. gloeosporioides* contributes significantly to pre- and post-harvest losses,[4] resulting in trade sanctions and barriers that affect agricultural markets.

This species thrives in a tropical environment where it can act as a primary pathogen (parasite), survive on decaying plant matter (saprophyte), or remain asymptomatically within plant tissues as an endophyte. Its capacity to afford several survival modes or lifestyles has sparked considerable interest among researchers, who seek to understand its ecological roles and behavior under controlled conditions. This curiosity highlights the potential of harnessing *C. gloeosporioides* not only as a pathogen but also as a source for discovering new biologically active compounds with significant economic importance.[5-9]

Various strategies have been employed to replicate the natural fungal environment to uncover these compounds, including classical axenic cultivation and more recent co-cultivation approaches using different solid and liquid media. The choice of media can significantly influence fungal growth and metabolite production, as certain pathogens exhibit preferences that are evident in their growth patterns. Replicating the complex dynamics of biotic and abiotic factors found in natural habitats presents a challenge; however, key parameters such as media type, pH, temperature, humidity, nutrient availability, and light conditions are critical for the growth and metabolic activity of fungi. Adjusting these factors can activate cryptic biosynthetic gene clusters (BGCs), potentially leading to the discovery of previously unidentified metabolites.[10]

In this study, we focus on exploring the chemo-diversity of secondary metabolites produced by *C. gloeosporioides* in different culture environments, specifically rice and potato dextrose broth (PDB). Previous research[11-15] has identified bioactive secondary metabolites from *C. gloeosporioides*, including neuroprotective glycosylated cyclic lipodepsipeptides and anticancer compounds like taxol. Although chaetiacandin-type compounds have been reported,[16] their bioactivity remains underexplored, with

*e-mail: pcvieira@fcfrp.usp.br
Editor handled this article: Hector Henrique F. Koolen (Associate)

limited evidence of anti-inflammatory or adiponectin-secretion-promoting activities. Investigating their antimicrobial properties could reveal novel applications against fungal or bacterial pathogens.

This research aims to elucidate how different cultivation media affect the secondary metabolite profiles of *C. gloeosporioides*, providing insights into the relationship between growth conditions and the production of bioactive compounds with potential antifungal activities.

Experimental

C. gloeosporioides cultivation and extraction

The fungal strain of *C. gloeosporioides* was commercially obtained from the microorganism collection of the Instituto Biológico do Estado de São Paulo and maintained in the laboratory collection. The strain was transferred to Petri dishes containing PDA (potato dextrose agar) medium and incubated for growth over 7 days. After this period, 6 mycelial discs of the fungi, each 0.5 cm in diameter, were transferred to 500 mL Erlenmeyer flasks containing 90 g of rice and 90 mL of distilled water. The cultivation was carried out with 6 Erlenmeyer flasks for 21 days, in the absence of light and under static conditions. After this period, extraction was performed using 150 mL of ethyl acetate for each Erlenmeyer flask, macerated with a glass rod, and subjected to ultrasound for 5 min, then filtered using a Buchner funnel and vacuum system. This process was repeated three times for each Erlenmeyer flask. Ethyl acetate was removed using a rotary evaporator under reduced pressure, yielding 1.59 g of crude extract.

The cultivation in PDB medium was conducted as described by Mazucato and Vieira,[17] where six mycelial discs of the fungi were transferred to 500 mL Erlenmeyer flasks containing 200 mL of PDB medium, totaling 6 Erlenmeyer flasks. The cultivation was carried out for 28 days under static conditions and without light. After this period, the medium was filtered as described previously, and the broth from each Erlenmeyer flask containing 200 mL PDB was extracted three times with 100 mL of ethyl acetate. The organic phase was rotary evaporated under reduced pressure, generating 32.24 mg of crude extract. The crude extract was analysed using 1D and 2D nuclear magnetic resonance spectroscopy (NMR) and gas chromatography-mass spectrometry (GC-MS).

NMR, mass spectroscopic and GC-MS analyses

1D and 2D NMR spectra were obtained at frequencies of 400 MHz (using a DRX-400, Bruker Advance) and 500 MHz (DRX-500, Bruker). The solvents utilized for these analyses included methanol-d_4, dimethylsulfoxide-d_6 (DMSO), and acetone-d_6.

High-resolution mass spectra were recorded on a micrOTOF-II mass spectrometer (Bruker Daltonics), which features an electrospray ionization (ESI) source coupled with a time-of-flight (TOF) analyzer. An infusion pump (KD Scientific) was used to deliver the sample at a rate of 0.20 mL h^{-1}. The measurements were carried out in positive ionization mode, with a drying gas flow rate of 7 L min^{-1} and a pressure of 2 bar, maintained at a temperature of 180 °C. The electrospray source was set to a capillary voltage of 3.0 kV and an end-plate voltage of 0.45 kV.

GC-MS analyses were performed using a Shimadzu QP2010Plus system (Shimadzu Corporation), which included an AOC-20i automatic injector and an electron ionization source (EI-EM) operating at 70 eV. The chromatographic separation was achieved using a fused silica Rtx5-MS capillary column (Restek), with dimensions of 30 m × 0.25 mm internal diameter and a 0.25 μm film thickness. Helium served as the carrier gas, flowing at a constant rate of 1.1 mL min^{-1}. The injector and ion source temperatures were both maintained at 200 °C. Samples were prepared in high-purity solvents (spectroscopic grade, J.T. Baker), with an injection volume of 1.0 μL. The oven temperature program started at 60 °C and increased to 280 °C at a rate of 10 °C min^{-1}.

Fractionation of rice medium extract

The crude extract (1.59 g) from the rice medium was initially fractionated by vacuum liquid chromatography (VLC) using a 350 mL glass column and flash silica (230-400 mesh). The extract was adsorbed on silica and transferred to the top of the column. The mobile phase consisted of a polarity gradient using 150 mL for each fraction. In total, 6 fractions were collected: 100% hexane (Hex), 66% hexane and 33% ethyl acetate (EtOAc), 33% hexane and 66% ethyl acetate, 100% ethyl acetate, 100% acetone (Ac), and 100% methanol, to afford six sub-fractions (ARF6.1-6.6). Subsequently, these fractions were separated by silica column chromatography using isocratic solvent (Hex:EtOAc:Ac 40:30:30) system as eluent and followed by a size-exclusion chromatography using Sephadex LH20 column (Amersham Pharmacia Biotech AB) with methanol as the eluent. The sub-fractions were managed/pull together via thin layer chromatography (TLC). The promising sub-fraction was later subjected to preparative thin layer chromatography (PTLC) using Hex:EtOAc:Ac 40:30:30 system as eluent to afford the sub-fractions ARF(6A-6C).

Finally, the sub-fractions were purified using a high-performance liquid chromatography (HPLC) system, which included an LC-6AD (Shimadzu) paired with a diode array detector (HPLC-DAD, SPD-M10AVP, Shimadzu). The column used was a Supelco C-8 semi-preparative with dimensions of 250 cm × 10 mm and a particle size of 10 µm. The mobile phase consisted of water and methanol, delivering 300 µL of sample injection volume at a flow rate of 4.0 mL min^{-1}.

Sub-fraction ARF6A, with a concentration of 22.4 mg in 300 µL, was subjected to fractionation using semi-preparative HPLC-DAD. This amount was injected as a single load, with the mobile phase consisting of water and methanol. The methanol gradient was ramped from 10 to 100% over 15 min, held at 100% for 2 min, then returned to 10% MeOH for 5 min to condition the column for the next injection for a total run time of 25 min. Compound **1** (colletotricandin A) was detected at 280 nm in 15.5 min of run time. This process resulted in the separation of compound **1** (14.9 mg).

A similar procedure was performed with slightly adjusting the binary gradient solvent system from 30 to 100% to afford compounds **2** and **3** (colletotricandin C and D).

Colletotricandin C (**2**) was isolated as a colorless paste, yielding 3.7 mg with an absorption peak at 280 nm in 12.3 min of run time. Colletotricandin D (**3**) was obtained as a colorless paste, yielding 2.2 mg, with an absorption peak at 300 nm in 16.7 min of run time. Thielavin U (**4**) was acquired as an amorphous solid, producing 26.7 mg with an absorption peak at 254 nm in 16.5 min of run time. Thielavin V (**5**), on the other hand, was obtained as a precipitate that was somewhat insoluble in methanol during the clean-up process prior to the HPLC injection of the sub-fraction from which thielavin U was isolated.

Antifungal activity

The samples were diluted in DMSO to a concentration that was 100 times the maximum level used in the testing. These dilutions were further prepared to achieve a 2 times concentration of the test substance in Roswell Park Memorial Institute (RPMI) 1640 culture medium (pH 7.0), supplemented with glutamine, devoid of bicarbonate, and containing phenol red as a pH indicator. The concentration ranges for testing the isolated substances spanned from 0.40 to 200 µg mL^{-1}.

Minimum inhibitory concentration (MIC) tests were conducted in accordance with the protocols established in M27-A3 and M38-A2 by the Clinical Laboratory Standards Institute (CLSI).[18,19] Each 2-times concentrated test solution (100 µL) was aliquoted into a 96-well microdilution plate, with columns 1 and 12 designated as positive (normal fungal growth) and negative (culture medium sterility) controls, respectively. Columns 2 through 11 received serial dilutions (1:2) of the test sample. Duplicate tests were performed on separate microdilution plates.

The MIC experiments were conducted using the filamentous fungi *Aspergillus flavus* (LMC23011) and *Fusarium falciforme* (LMC23007.2), as well as the yeast-like fungi *Candida albicans* (ATCC64548) and *Candida parapsilosis* (ATCC22019). Suspensions of the fungi were prepared according to the standardized methodology. After incubation, the fungal cell suspensions were adjusted to a uniform concentration and inoculated into the microdilution plates. Incubation was performed at 37 °C, with readings taken at 24 and 48 h to determine the MIC.

Results and Discussion

Compound **1** was isolated as an amorphous powder. Its structure was determined by comparison of its ^{1}H NMR (Figure S1, Supplementary Information (SI) section) with data obtained from literature[15] as shown in Table S1, (SI section) and Figure 1.[6] In the ^{1}H NMR spectrum, the signals at δ_H 5.09, 4.81, 3.95, 3.69, and 3.51 are diagnostic of a sugar moiety in the molecule. In addition, the protons represented by signals at δ_H 6.27 and 6.40 are characteristic of an aromatic ring with *meta*-coupled hydroxyl substitution. The δ_H 6.98, 5.89 5.35, and 5.30, with *J* couplings of 15 Hz are typical of olefinic protons along with δ_H 2.39, 2.14, 2.06, 1.97, 1.29, and 0.86 assigned to protons on the side chain in the molecule. Based on this information and the data reported in the literature, this compound was identified as colletotricandin A (**1**).

The structural determination of compound **1** is included to underscore the uniqueness of the newly synthesized compounds, emphasizing that differences primarily stem from hydroxyl substitutions on the alkyl chain, while the core structure remains intact. This comparison is crucial for illustrating structural variations and confirming the novelty of the new derivatives.

Compound **2** was isolated as a colorless paste, and its molecular formula ($C_{25}H_{36}O_{10}$) was determined by high-resolution electrospray ionization mass spectrometry (HRESIMS, Figure S2, SI section), as observed by *m/z* 519.2187 $[M + Na]^+$ (calcd. for $C_{25}H_{36}O_{10}Na^+$, 519.2201) with an error of –2.7 ppm, and ^{1}H NMR (Figure S3, SI section). Signals similar to those of compound **1** (Table S1, SI section) were observed, as shown in Table 1, suggesting a derivative of this compound. However, differences were

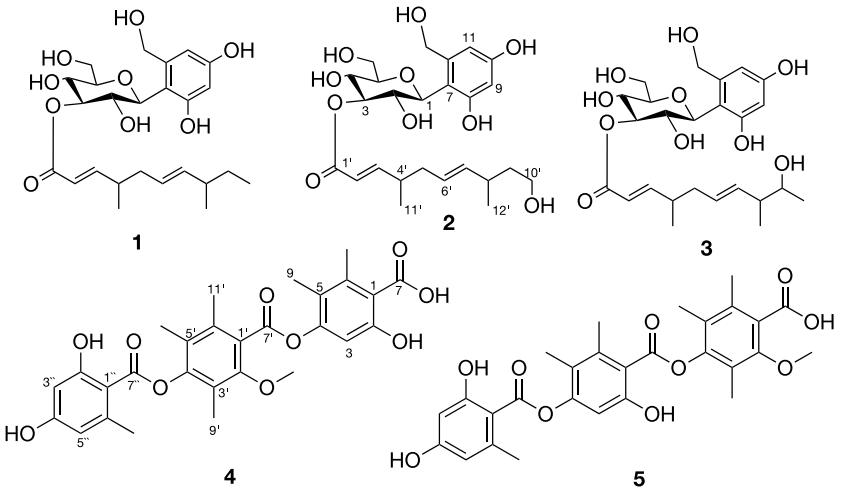

Figure 1. Metabolites from axenic culture of *C. gloeosporioides* in rice medium.

observed due to the absence and change in multiplicities of the terminal methyl signal $\delta_{H10'}$ 0.86 ppm and the methylene protons $\delta_{H9'}$ 1.29 (Table S1, SI section), of the side chain in compound **2**, suggesting a change in position 10'. This change was confirmed by observing the proton $\delta_{H10'}$ 3.50, which overlapped with the proton δ_{H5} 3.50, confirmed by heteronuclear single-quantum correlation (HSQC, Figure S4, SI section), indicating hydroxylation at position 10'. Using ^{1}H–^{1}H correlation spectroscopy (COSY), proton sequences in the sugar moiety and proton correlations in the side chain were established, as shown in Figure S5 (SI section). Employing the heteronuclear multiple-bond correlation (HMBC) technique (Figure S6, SI section), correlations of δ_{H1} with carbons at positions C-8, C-12, δ_{H13} with C-11, δ_{H11} with C-12, C-10, and C-9, δ_{H3} with C-1', $\delta_{H11'}$ with C-3', $\delta_{H12'}$ with C-7' and C-9' were observed, connecting all parts of the molecule. The correlation of $\delta_{H10'}$ with C-9' and C-8' was crucial to confirm the hydroxylation at position C-10' of the molecule (Figure 2). Since there were no other differences in the ^{1}H NMR spectrum, the compound was assigned as a new derivative of colletotricandin A and, thus, named colletotricandin C (**2**).

Compound **3** was isolated as a colorless paste and its molecular formula ($C_{25}H_{36}O_{10}$) was determined by HRESIMS (Figure S7, SI section) as observed by 519.2200 *m/z* $[M + Na]^+$ (calcd. for $C_{25}H_{36}O_{10}Na^+$, 519.2201) with an error of –0.2 ppm. A comprehensive analysis of the ^{1}H NMR (Figure S8, SI section) and HSQC (Figure S9, SI section) spectra of compound **3**, along with comparisons to the spectral data for compounds **1** and **2**, reveals that these compounds are colletotrichandin derivatives. Specifically, hydroxylation occurs at position C-9' in compound **3**, which differentiates it from compound **2** (Table 1). This can be observed by analyzing the proton at $\delta_{H9'}$ 3.50, which overlaps with the signal at δ_{H5} 3.50, but unlike compound **2**, these signals integrate for 2 protons. This was confirmed by HSQC and the fact that the methyl group $\delta H_{10'}$ 1.08, 3H, d (6.3) shows a doublet coupling. The ^{1}H–^{1}H COSY (Figure S10, SI section) and HMBC (Figure S11, SI section) correlations, which were crucial for determining the connectivity of the structure, are shown in Figure 3. Therefore, compound **3** was identified in this study as the second derivative of colletotrichandin A and was named colletotrichandin D.

Compound **4** was isolated as an amorphous powder. Its molecular formula ($C_{28}H_{28}O_{10}$) was determined by ^{1}H NMR (Figure S12, SI section) and HRESIMS (Figure S13, SI section) with 547.1559 *m/z* $[M + Na]^+$ (calcd. for $C_{28}H_{28}O_{10}Na^+$, 547.1575) with an error of –2.9 ppm, and comparison with literature data as shown in Table 2. The protons at δ_H 7.05, 2.69, and 2.00 showed HMBC correlations with six aromatic ring carbons δ_C 117.2, 161.8, 105.6, 150.0, 117.9, and 140.9 (Figure S14, SI section), indicating their connectivity in the system as shown in Figure 4. The protons at δ_H 2.13, 2.12 and 2.16 correlated with other aromatic ring carbons, along with the methoxyl group δ_H 3.70, being δ_C 127.1, 153.2, 121.8, 149.5, 125.9, and 132.3. Finally, the signals at δ_H 6.67, 6.61 and 2.61 correlated with a third aromatic ring δ_C 107.52, 162.0, 100.71, 159.15, 110.4, and 141.1. The *para*-substituted ester linkage between the rings in compound **4** was confirmed by comparing its chemical shift data with literature[20] values, particularly those of thielavins and colletotric acid, which exhibit *meta*-substitution. The observed chemical shifts were consistent with *para* substitution, as seen in thielavins. After analyzing the signals, compound **4** was identified as a new derivative of thielavin, named 3-demethylthielavin M. Subsequently, compound **5** was characterized using the same comparative

Table 1. ^{1}H and ^{13}C NMR (500 MHz, CD_3OD) spectroscopic data for compounds **2** and **3**

Position	Colletotricandin C (**2**)		Colletotricandin D (**3**)	
	δ_H / ppm, H, mult. (*J* / Hz)	δ_C / ppm	δ_H / ppm, H, mult. (*J* / Hz)	δ_C / ppm
1	4.80, 1H, d (9.6)	77.05	4.84, 1H, d (9.5)	76.82
2	3.95, 1H, t (9.6)	70.45	3.95, 1H, t (9.7)	70.11
3	5.09, 1H, t (9.4)	79.65	5.09, 1H, t (9.4)	79.92
4	3.69, 1H, t (9.6)	69.04	3.69, 1H, t (9.7)	68.22
5	3.50, 1H, m	81.17	3.51, 1H, m	80.99
6a	3.86, 1H, dd (12.1, 2.2)	60.95	3.86, 1H, dd (12.1, 2.3)	60.55
6b	3.78, 1H, dd (12.1, 4.5)		3.78, 1H, dd (12.1, 4.6)	
7		112.69		112.9
8		157.35		157.22
9	6.26, 1H, d (2.5)	102.48	6.27, 1H, d (2.6)	102.46
10		157.42		157.83
11	6.40,1H, d (2.5)	107.7	6.40,1H, d (2.6)	107.76
12		141.07		141.16
13a	4.64, 1H, d (12.3)	62.00	4.63, 1H, d (12.4)	61.95
13b	4.55, 1H, d (12.3)		4.55, 1H, d (12.4)	61.87
1’		165.9		166.8
2’	5.88, 1H, dd (15.7, 1.2)	119.84	5.88, 1H, dd (15.8, 1.3)	120.14
3’	6.93, 1H, dd (15.7, 7.4)	154.07	6.95, 1H, dd (15.7, 7.5)	154.45
4’	2.40, 1H, sept (6.9)	35.85	2.41, 1H, sept (6.8)	35.55
5’a	2.22, 1H, quint (7.4)	39.03	2.13, 1H, m	38.88
5’b	2.11, 1H, m		2.11, 1H, m	
6’	5.35, 1H, dd (15.3, 6.4)	125.75	5.40, 1H, m	125.83
7’	5.28, 1H, t (9,3)	138.25	5.41, 1H, m	134.73
8’	2.09, 1H, m	33.42	2.09, 1H, m	44.12
9’	1.47, 2H, m	39.56	3,50, 1H, m	70.35
10’	3.50, 2H, m	60.34	1.08, 3H, d (6.3)	19.38
11’	1.07, 3H, d (6.7)	17.45	1.06, 3H, d (6.7)	16.45
12’	0.98, 3H, d (6.9)	20.22	1.00, 3H, d (6.9)	15.05

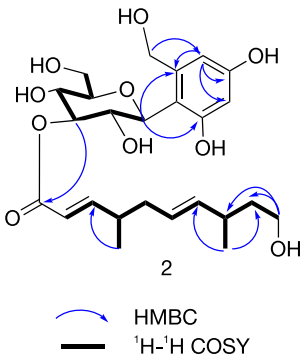

Figure 2. 2D NMR correlations of the new colletotrichandin **2**.

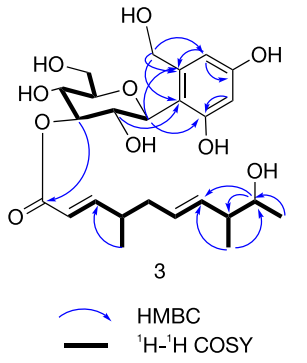

Figure 3. 2D NMR correlations of the new colletotrichandin **3**.

approach with data from existing literature.[21] All relevant data are presented in Table 2.

Compound **5** was isolated as an amorphous solid. The ^{1}H NMR analysis (Figure S15, SI section) showed a compound very similar to compound **4**, which was confirmed by HRESIMS (Figure S16, SI section) with the same molecular mass and formula given as $C_{28}H_{28}O_{10}$ with 547.1569 *m/z* $[M + Na]^+$ (calcd. for $C_{28}H_{28}O_{10}Na^+$, 547.1575) with an error of –1.1 ppm. The compound showed protons at δ_H 7.10, 6.81, 6.70, 3.72, 2.61, 2.60,

Table 2. ^{1}H and ^{13}C NMR spectroscopic data for compounds **4** and **5**

Position	3-Demethylthielavin M (**4**)[a]		Compound **5**[b]		3'',3'-Didemethyl-3-methylthielavin N (**5**)[a]	
	δ_H / ppm, H, mult. (*J* / Hz)	δ_C / ppm	δ_H / ppm, H, mult. (*J* / Hz)	δ_C / ppm	δ_H / ppm, H, mult. (*J* / Hz)	δ_C / ppm
1		117.2		115.1		126.5
2		161.8		159.7		132.2
3	6.35, 3H, br s	105.6	–	–		125.9
4		150.0		151.9		149.7
5		117.9		120.7		122.1
6		140.9		138.1		153.3
7		172.4		175.6		not observed
8	2.61, 3H, s	17.60	2.62 (3H, s)	18.7	3.78, 3H, s	62.0
9	2.05, 3H, s	11.9	2.00 (3H, s)	13.1	2.14, 3H, s	10.0
10	–	–	–	–	2.13, 3H, s	12.8
11	–	–	–	–	2.31, 3H, s	16.5
1'		127.1		127.2		122.4
2'		153.2		154.9		152.4
3'		121.8		122.7	6.60, 1H, s	106.9
4'		149.5		149.4		149.2
5'		125.9		126.5		119.21
6'		132.3		133.9		135.5
7'		not observed		166.5		169.6
8'	3.76, 3H, s	62.3	3.71 (3H, s)	62.3	2.21, 3H, s	16.8
9'	2.13, 1H, br s	9.9	2.14 (3H, s)	10.04	2.08, 3H, s	11.4
10'	2.12, 3H, s	12.70	2.00 (3H, s)	13.1	–	–
11'	2.30, 3H, s	16.5	2.25 (3H, s)	17.3	–	–
1''		107.52		104.9		107.7
2''		162.0		166.1		159.6
3''	6.29, 1H, br s	100.71	6.71 (1H, d)	102.2	6.27, 1H, br s	100.66
4''		159.15		165.0		161.5
5''	6.27, 1H, d, (2.2)	110.4	6.64 (1H, d)	113.2	6.26, 1H, br s	110.23
6''		141.1		144.0		141.08
7''		167.52		169.6		167.8
8''	2.39, 3H, s	21.79	2.44 (3H, s)	10.4	2.39, 3H, s	21.77
OH	10.60	–	–	–	10.52	–
OH	10.25	–	–	–	10.13	–

[a]Measured in 500 MHz, pyridine-d_5; [b]NMR data previously published for compound **5** measured in pyridine-d_5.[21]

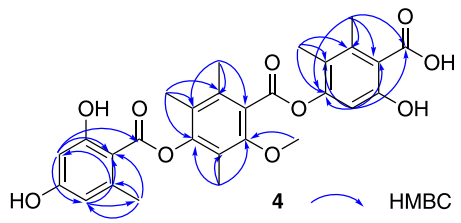

Figure 4. HMBC correlations of the new thielavin **4**.

2.19, 2.18, 2.14, and 2.00 (Table 2), which were connected by HMBC (Figures S17 (SI section), and 5), and following the same signal assignment, it was realized that this compound slightly differs from compound **4**. The spectrum of compound **4** exhibited the same core with identical chemical shifts for the δ_H 3'', 5'', and 8'' signals (Table 2), indicating that there was no alteration in the third core. Slight differences in chemical shifts were observed in the other two cores. Compound **4** exhibited a proton resonance at δ_H 7.05, while the corresponding proton (δ_H 3') in compound **5** appeared at a slightly upfield shift of δ_H 7.01, probably due to their different environments, despite the two compounds showing similar HMBC correlations. Another example is δ_{H8} at 2.69, corresponding to $\delta_{H8'}$ at 2.61 of compound **5**, which also showed similar correlations in the HMBC (Figure 5). The resemblance in the HMBC

and mass spectrum, along with differences only in the chemical shifts of certain hydrogens as observed in Table 2, suggest that there were no changes in the structure of the compound but only in the chemical environment of some hydrogens. Therefore, these structures were attributed to different configurations. Thus, it was identified as another new derivative of thielavin, named 3",3'-didemethyl-3-methylthielavin N (**5**).

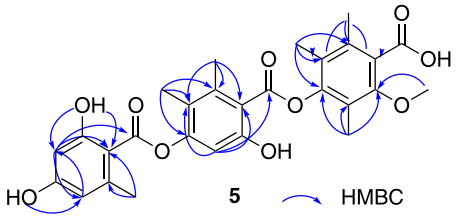

Figure 5. HMBC correlations of the new thielavin **5**.

Media comparative analysis

A comparative analysis of the chemical diversity of cultivating *C. gloeosporioides* in rice and PDB media, utilizing techniques such as NMR and GC-MS, provides a comprehensive understanding of fungal media preferences and their induced behaviors. This analysis is essential for advancing fungal research, particularly in identifying overlooked features of microbial expression across different media set ups and for facilitating the production of specialized metabolites.

Comparative analysis of rice and PDB crude extracts using ^{1}H NMR

The ^{1}H NMR spectra of *C. gloeosporioides* extracts from rice and PDB reveal signals in the downfield region (δ_H 7.40-6.45) that are characteristic of aromatic protons, including a mixture of metabolites (Figures S18 and S19, SI section). The ^{1}H NMR spectrum of rice (Figure S18), reveals resonances in the range of δ_H 5.40-4.20, which are typical of oxygenated (sp^2) protons. Additionally, a signal at δ_H 11.50 suggests a chelated hydroxyl-proton, commonly found in molecules with adjacent hydroxyl and carbonyl groups in a delocalized pi-electron system. The upfield regions displayed resonances of alkyl (sp^3) protons in electron-deficient environments. The use of various chromatographic techniques enabled the isolation and characterization of compounds **1**-**5** from the rice extract.

In contrast, the ^{1}H NMR spectrum of the PDB extract displayed fewer signals (Figure S19), indicating lower chemical diversity and reduced compatibility with the substrate. Notably, distinct signals at δ_H 3.77 (2H, t, *J* 7.10 Hz) and 2.82 (2H, t, *J* 7.08 Hz), along with resonances integrating for 5H at δ_H 7.36-7.16, suggest the presence of a mono-substituted aromatic ring, identified as 2-phenyletan-1-ol. This compound is a precursor to *N*-phenethylacetamide, detected via GC-MS at 19.3 min in the mid-polar fraction, see Figure 6. The NMR spectrum (Figure S19) also displayed signals at δ_H 6.71 (2H, d, *J* 8.5 Hz) and δ_H 7.05 (2H, d, *J* 8.5 Hz), characteristic of tyrosol, which was further confirmed by GC-MS at a retention time of 19.3 min (2.51%). These findings indicate that both analytical methods corroborate the identification of tyrosol in the PDB extracts.

Comparative analysis of rice and PDB crude extracts using GC-MS

GC-MS primarily targets volatile constituents in extracts, predominantly in the non-polar and mid-polar fractions. Stratifying extracts based on the solvents used (hexane for non-polar and ethyl acetate for mid-polar), enhances spectral resolution and elucidates metabolites profiles (Figures S20-S34, SI section). The mid-polar fraction containing tyrosol and *N*-phenethylacetamide were detected at retention times of 19.3 min (2.51%) and 20.9 min (1.27%), respectively. *N*-Phenethylacetamide exhibits papain inhibitory activity of 89% at 200 μM.[17]

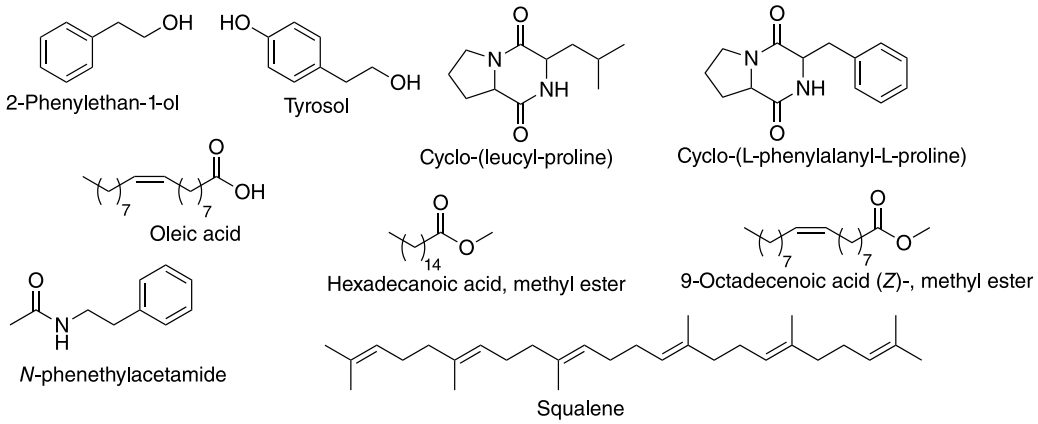

Figure 6. Compounds identified by GC-MS.

Diketopiperazine isomers, specifically cyclo-(L-leucyl-L-prolines), were identified at retention times of 26.7, 28.4, and 28.7 min, with area peaks of 9.91, 11.53, and 15.47%, respectively, indicating their stereoisomeric nature. Cyclo-(L-phenylalanyl-L-proline) isomers were detected at 34.7 min (2.01%) and 35.4 min (21.46%) (Figures S26-S30, SI section). These diketopiperazines differ only in their amino acid composition, leucine or phenylalanine, while the cyclo-proline structure remains unchanged. These metabolites are recognized for their strong antioxidant activity,[22,23] and are essential for fungal growth and ecological interactions.

The PDB non-polar fractions revealed several metabolites, notably hexadecanoic acid, methyl ester (14.05%), and 9-octadecenoic acid (*Z*)-, methyl ester (16.42%), identified as the predominant constituents. These fatty acids methyl esters (FAMEs) are reported[24] to exhibit antibacterial and anticandidal activities. In contrast, the rice extract contained oleic acid (18.24%) and squalene (61.37%), as the most abundant components in the non-polar and mid-polar fractions, with squalene noted for its cardio-protective effects, while the activities of mono-unsaturated fatty acids are well documented.[25]

In addition to these major constituents, various pharmacologically active compounds were identified at lower concentrations. The synergistic effects of these metabolites may significantly influence the survival of organisms and interactions with other microbes within their ecosystems. This direct GC-MS method provides reliable and reproducible quantitative results.[24] The observed differences in chemical composition and yield underscore the importance of utilizing different media to study fungi, allowing for the identification of distinct metabolites and providing a profile of chemical diversity.

Antifungal activity

The preliminary antifungal activity of compounds **1**-**5** was evaluated against two human pathogens, *C. albicans* and *C. parapsilosis*, as well as two plant pathogens, *Aspergillus flavus* and *Fusarium solani*. None of the compounds demonstrated significant antifungal activity against these strains, raising important questions about the potential applications of these newly identified metabolites for addressing phytopathogenic and human pathogenic challenges.

The absence of antifungal activity may suggest that the structural characteristics of these compounds are not conducive to combating the tested strains or that they possess a specific mode of action not captured in this initial screening. This highlights the necessity for further exploration of their biological activities and a reassessment of the extraction and screening methodologies to enhance the recovery of bioactive compounds. While the current findings do not support the antifungal efficacy of compounds **1**-**5**, they open promising avenues for further investigation that could lead to novel antifungal strategies.

Conclusions

Colletotrichum gloeosporioides is a notable phytopathogen, and this study highlights significant differences in its chemical diversity when cultured in various media, particularly rice. The use of ^{1}H NMR and GC-MS techniques revealed that the rice medium not only enhanced the yield but also increased the chemical diversity of metabolites, leading to the identification of four new compounds: colletotricandin C and D, along with thielavin U and V. This comparative approach demonstrates a cost-effective and time-efficient method for metabolite analysis across different culture conditions, although it demands considerable expertise.

Despite these promising findings, the antifungal assays against *Candida albicans*, *Candida parapsilosis*, *Aspergillus flavus*, and *Fusarium solani*, showed no activity. This lack of activity raises questions about the potential applications of the newly identified metabolites in combating phytopathogenic and human pathogenic strains. Future studies should expand the range of strains tested, particularly resistant strains, and investigate different experimental conditions to better elucidate their therapeutic potential. Overall, this study underscores the importance of media choice in metabolite production and invites further exploration of the ecological and pharmacological roles of these newly discovered compounds.

Supplementary Information

Supplementary information (1D and 2D NMR spectra, HRESIMS and GC-MS chromatograms) is available free of charge at http://jbcs.sbq.org.br as PDF file.

Acknowledgments

M. N. A., V. S. M., and P. C. V. express their gratitude to Faculdade de Ciências Farmacêuticas de Ribeirão Preto at Universidade de São Paulo (FCFRP-USP) for providing an enabling environment and access to research facilities. M. N. A. also extends appreciation to Federal College of Education (Technical) Gusau for granting a leave of absence. This work was funded by Fundação de Amparo à Pesquisa do Estado de São Paulo (FAPESP, Brazil), through

the researchers at risk-initiative (grant No. 13/07600-3 and No. 22/10835-1), Coordenação de Aperfeiçoamento de Pessoal de Nível Superior (CAPES, finance code 001), and Conselho Nacional de Desenvolvimento Científico e Tecnológico (CNPq).

References

1. Chowdhury, M. N. A.; Rahim, M. A.; *J. Agric. Rural Dev.* **2009**, *7*, 115. [Crossref]
2. Ploetz, R. C.; Freeman, S. In *The Mango: Botany, Production and Uses*; Litz, R. E., ed.; CABI: Wallingford, UK, 2009, p. 232. [Link] accessed in February 2025
3. Bally, I. S.; Hofman, P. J.; Irving, D. E.; Coates, L. M.; Dann, E. K.; *Acta Hortic.* **2006**, *820*, 365. [Crossref]
4. Jenny, F.; Sultana, N.; Islam, M.; Khandaker, M. M.; Bhuiyan, M. A. B.; *Bangladesh J. Plant Phytopathol.* **2019**, *35*, 65. [Link] accessed in February 2025
5. Ajay, K. G.; *J. Plant Physiol. Pathol.* **2014**, *2*, 2. [Crossref]
6. Liu, H. X.; Tan, H. B.; Chen, Y. C.; Li, S. N.; Li, H. H.; Zhang, W. M.; *Nat. Prod. Res.* **2018**, *32*, 2360. [Crossref]
7. Sharma, V. K.; Kumar, J.; Singh, D. K.; Mishra, A.; Verma, S. K.; Gond, S. K.; Kumar, A.; Singh, N.; Kharwar, R. N.; *Front. Microbiol.* **2017**, *8*, 1126. [Crossref]
8. Song, J. H.; Lee, C.; Lee, D.; Kim, S.; Bang, S.; Shin, M. S.; Lee, J.; Kang, K. S.; Shim, S. H.; *J. Nat. Prod.* **2018**, *81*, 1411. [Crossref]
9. Bang, S.; Lee, C.; Kim, S.; Song, J. H.; Kang, K. S.; Deyrup, S. T.; Nam, S. J.; Xia, X.; Shim, S. H.; *J. Org. Chem.* **2019**, *84*, 10999e. [Crossref]
10. Skellam, E.; Rajendran, S.; Li, L.; *Commun. Chem.* **2024**, *7*, 89. [Crossref]
11. Balaji, V.; Ebenezer, P.; *Indian J. Sci. Technol.* **2008**, *1*, 1. [Link] accessed in February 2025
12. Nithya, K.; Muthumary, J.; *Recent Res. Sci. Technol.* **2011**, *3*, 44. [Link] accessed in February 2025
13. Arivudainambi, U. S. E.; Anand, T. D.; Shanmugaiah, V.; Karunakaran, C.; Rajenrdan, A.; *FEMS Immunol. Med. Microbiol.* **2011**, *61*, 340. [Crossref]
14. Amirita, A.; Sindhu, P.; Swetha, J.; Vasanthi, N. S.; Kannan, K. P.; *World J. Sci. Technol.* **2012**, *2*, 13. [Link] accessed in February 2025
15. Lee, C.; Gong, J.; Kim, J.; Ko, H.; An, S.; Bang, S.; Shim, S. H.; *J. Nat. Prod.* **2022**, *85*, 501. [Crossref]
16. Silva, T. L.; Toffano, L.; Fernandes, J. B.; Silva, M. F. G. F.; Sousa, L. R. F.; Vieira, P. C.; *Braz. J. Microbiol.* **2020**, *51*, 1169. [Crossref]
17. Mazucato, V. S.; Vieira, P. C.; *Nat. Prod. Res.* **2023**, *37*, 3947. [Crossref]
18. Clinical and Laboratory Standards Institute; *M27-A3: Reference Method for Broth Dilution Antifungal Susceptibility Testing of Yeasts*, 3rd ed.; CLSI: Pennsylvania, 2008. [Link] accessed in February 2025
19. Clinical and Laboratory Standards Institute; *M38-A2: Reference Method for Broth Dilution Antifungal Susceptibility Testing of Filamentous Fungi*, 2nd ed.; CLSI: Pennsylvania, 2008. [Link] accessed in February 2025
20. Zou, W. X.; Meng, J. C.; Lu, H.; Chen, G. X.; Shi, G. X.; Zhang, T. Y.; Tan, R. X.; *J. Nat. Prod.* **2000**, *63*, 1529. [Crossref]
21. Sakemi, S.; Hirai, H.; Ichiba, T.; Inagaki, T.; Kato, Y.; Kojima, N.; Nishida, H.; Parker, J. C.; Saito, T.; Tonai-Kachi, H.; VanVolkenburg, M. A.; *J. Antibiot.* **2002**, *55*, 941. [Crossref]
22. Ser, H. L.; Palanisamy, U. D.; Yin, W. F.; Abd Malek, S. N.; Chan, K. G.; Goh, B. H.; Lee, L. H.; *Front. Microbiol.* **2015**, *6*, 158812. [Crossref]
23. MubarakAli, D.; Praveenkumar, R.; Shenbagavalli, T.; Nivetha, T. M.; Ahamed, A. P.; Al-Dhabi, N. A.; Thajuddin, N.; *RSC Adv.* **2012**, *2*, 11552. [Link] accessed in February 2025
24. Ryan, E.; Galvin, K.; O'Connor, T. P.; Maguire, A. R.; O'Brien, N. M.; *Int. J. Food Sci. Nutr.* **2006**, *57*, 19. [Crossref]
25. Ai, J.; *J. Agric. Food Chem.* **1997**, *45*, 3932. [Crossref]

Submitted: December 18, 2024
Published online: March 12, 2025